Experimental Neurology 311 (2019) 305–312

Contents lists available at ScienceDirect

Experimental Neurology

journal homepage: www.elsevier.com/locate/yexnr

Research Paper

Defective daily temperature regulation in a mouse model of amyotrophic lateral sclerosis

Maurine C. Braun[a,1], Alexandra Castillo-Ruiz[a,2], Premananda Indic[a,3], Dae Young Jung[b], Jason K. Kim[b,c], Robert H. Brown Jr.[a,*], Steven J. Swoap[d], William J. Schwartz[a,**,4]

[a] Department of Neurology, University of Massachusetts Medical School, Worcester, MA 01655, USA
[b] Program in Molecular Medicine, University of Massachusetts Medical School, Worcester, MA 01655, USA
[c] Division of Endocrinology, Metabolism, and Diabetes, Department of Medicine, University of Massachusetts Medical School, Worcester, MA 01655, USA
[d] Department of Biology, Williams College, Williamstown, MA 01267, USA

ARTICLE INFO

Keywords:
SOD1
G93A
Circadian
Suprachiasmatic nucleus
Scholander curves

ABSTRACT

Current understanding of the pathogenesis of the familial form of amyotrophic lateral sclerosis has been aided by the study of transgenic mice that over-express mutated forms of the human CuZn-superoxide dismutase (*SOD1*) gene. While mutant SOD1 in motor neurons determines disease onset, other non-cell autonomous factors are critical for disease progression, and altered energy metabolism has been implicated as a contributing factor. Since most energy expended by laboratory mice is utilized to defend body temperature (T_b), we analyzed thermoregulation in transgenic mice carrying the G93A mutation of the human *SOD1* gene, using implantable temperature data loggers to continuously record T_b for up to 85 days. At room (22 °C) ambient temperature, G93A mice exhibited a diminished amplitude of the daily T_b rhythm compared to C57BL/6J controls, secondary to decreased T_b values during the dark (behaviorally active) phase of the light-dark cycle. The defect arose at 85–99 days of age, around the age of symptom onset (as assessed by grip strength), well before observable weakness and weight loss, and could not be accounted for by decreased levels of locomotor activity or food consumption. Housing under thermoneutral (29 °C) ambient temperature partially rescued the defect, but age-dependently (only in animals > 100 days of age), suggesting that the deficit in older mice was due in part to inadequate thermogenesis by "peripheral" thermogenic organs as the disease progressed. In younger mice, we found that cold-induced thermogenesis and energy expenditure were intact, hinting that an initial "central" defect might localize to the subparaventricular zone, involving neural output pathways from the circadian clock in the hypothalamic suprachiasmatic nucleus to forebrain thermoregulatory circuitry.

1. Introduction

Research on familial forms of amyotrophic lateral sclerosis (ALS) – a disease characterized by progressive muscle weakness, atrophy, and spasticity due to the degeneration of upper and lower motor neurons (for review, see Brown and Al-Chalabi, 2017) – has led to significant insights into etiopathogenesis. The first genetic cause of familial ALS was identified in the CuZn-superoxide dismutase (*SOD1*) gene (Rosen et al., 1993), and hundreds of mutations across the SOD1 primary structure have now been found. The first mouse model of the disease

Abbreviations: ALS, amyotrophic lateral sclerosis; BAT, brown adipose tissue; T_b, body temperature; G93A, glycine 93 to alanine mutation; DMH, dorsomedial nucleus of the hypothalamus; HSF1, heat-shock factor 1; LD, light-dark; MMPC, National Mouse Metabolic Phenotyping Center; NDS, normal donkey serum; PBS, phosphate buffered saline; SCN, suprachiasmatic nucleus; SOD1, superoxide dismutase; SPZ, subparaventricular zone; UMMS, University of Massachusetts Medical School; ZT, *zeitgeber* time

* Correspondence to: R. H. Brown, Department of Neurology, University of Massachusetts Medical School, 55 Lake Avenue North, Worcester, MA 01655, USA.
** Correspondence to: W. J. Schwartz, Department of Neurology, Dell Medical School, Health Discovery Building, Suite 5.708, 1701 Trinity Street, Austin, TX 78712, USA.
E-mail addresses: robert.brown@umassmed.edu (R.H. Brown), william.schwartz@austin.utexas.edu (W.J. Schwartz).
[1] Current address: WAVE Life Sciences, Ltd., 733 Concord Avenue, Cambridge, MA 02138
[2] Current address: Neuroscience Institute, Georgia State University, Atlanta, GA 30303
[3] Current address: Dept. Electrical Engineering, College of Engineering, The University of Texas at Tyler, Tyler, TX 75799
[4] Current address: Depts. Neurology, Dell Medical School, and Integrative Biology, College of Natural Sciences, The University of Texas at Austin, Austin, TX 78712

https://doi.org/10.1016/j.expneurol.2018.07.008
Received 4 April 2018; Received in revised form 9 July 2018; Accepted 17 July 2018
Available online 18 July 2018
0014-4886/

(Gurney et al., 1994) followed transgenic overexpression of the entire human *SOD1* gene (*hSOD1*) with the glycine 93 to alanine mutation (G93A), under control of the endogenous *hSOD1* promoter. The G1 line of the G93A mouse, with 25 predicted copies of the transgene and backcrossed to C57BL/6, has become the most widely-used and intensively-studied animal model of the disease (see Kanning et al., 2010).

Murine models have been central to our current understanding of the pathogenesis of familial ALS. A toxic gain-of-function of the mutant protein underlies the death of motor neurons in the disease (Reaume et al., 1996), and several candidate mechanisms, not mutually exclusive, have been proposed, including mitochondrial dysfunction, protein aggregation, excitotoxicity, and dysregulated axonal transport (for review, see Taylor et al., 2016). While much research has focused on pathological mechanisms that act within the motor neuron itself to determine disease onset, non-neuronal cells and non-cell-autonomous pathways also contribute to disease expression and progression (for reviews, see Boillée et al., 2006; Ioannides et al., 2016). Most mutations in humans are associated with reduced SOD1 activity in some non-neural cell types (Robberecht et al., 1994; Tsuda et al., 1994), and in the G93A mouse there is actually considerably more of the mutated hSOD1 in liver and kidney than in spinal cord and brain (Zetterström et al., 2007).

Evidence for systemic metabolic dysregulation has been reported in transgenic mouse models that exhibit signs of a hypermetabolic state. Dupuis et al. (2004) (their Fig. 1) showed an approximate 16% increase in energy expenditure and 15% decrease in body weight in G93A mice at 75 days of age, compared to controls, while Lim et al. (2014) reported similar results at 120 days; in neither study was there a difference in food consumption from controls. For a small rodent housed at room temperature in a laboratory setting, much of the energy expended is utilized to defend body temperature (T_b) (Speakman, 1997), but there have been relatively few studies of T_b in ALS transgenic mice. To our knowledge, there has been no abnormality reported in baseline T_b in symptomatic G93A mice, as measured either during the light (rest) phase of the light-dark (LD) cycle (Weydt et al., 2006; Tankersley et al., 2007; Kandinov et al., 2011) or during a 24 h test session (Smittkamp et al., 2014). Only at a very late stage of the disease (> 130 days of age), are the mice unable to maintain T_b during cold stress (Kandinov et al., 2011).

Here we report our analysis of temperature regulation in G93A mice. We used implantable temperature data loggers (ibuttons) and continuously recorded T_b in animals for up to 85 days, at room (22 °C) or thermoneutral (29 °C) ambient temperatures; we also tested the animals' responsiveness to cold stress and generated plots of energy expenditure at various sub-thermoneutral ambient temperatures (Scholander curves; see Cannon and Nedergaard, 2011). The results revealed a defect expressed during the dark (behaviorally active) phase of the LD cycle, leading to a decreased amplitude of the daily T_b rhythm, the underlying mechanism(s) of which appeared to change as a function of age.

2. Materials and methods

2.1. Animals

Male transgenic mice carrying a G93A mutated *hSOD1* gene (B6·Cg-Tg(SOD1*G93A) 1Gur/J) and wild type (C57BL/6J) controls (initially obtained from Jackson Laboratories, Bar Harbor, ME) were individually housed in clear polypropylene cages contained within environmental compartments with ambient temperature held at 22 °C or 29 °C and relative humidity at 40 ± 20%. Food and water were provided ad libitum, and animals were maintained in a 12 h: 12 h LD cycle, with light intensity on the order of 300–400 lx at the mid-cage level. Locomotor activity was measured by passive infrared motion detectors (K-940, Visonic, Tel-Aviv, Israel) positioned on the top of the cages or by voluntary running in 5″ metal running wheels. Twice weekly, mice were weighed, tested for grip strength (as the maximum of 5 attempts using a Chatillon DFIS-2 Digital Force Gauge [Ametek, Inc., Berwyn, PA]), and given a neurological score according to the Jackson Laboratory criteria for onset and end stage of disease in G93A mice (Leitner et al., 2009); the endpoint of "death" was defined as an inability of the mouse to right itself within 15 s if laid on either side. At the conclusion of experiments, mice were euthanized using either ketamine (150 mg/kg) and xylazine (10 mg/kg) or CO_2 asphyxiation, followed by decapitation. Mutant *hSOD1* copy number was confirmed by PCR. All animal procedures were in accordance with the National Institutes of Health Guide for the Care and Use of Laboratory Animals and approved by the Institutional Animal Care and Use Committees of the University of Massachusetts Medical School (UMMS) and Williams College.

2.2. ibutton implantation, long-term recordings, and indirect calorimetry (UMMS)

ibuttons (DS1922L-F5, Embedded Data Systems, Lawrenceburg, KY) were calibrated at temperatures between 25 °C and 40 °C and then programmed to sample temperature every 15 min beginning at a specified age. They were coated lightly with paraffin wax and sterilized in povidine iodine solution overnight followed by a sterile saline rinse. At 38 days of age, mice were anesthetized with isoflurane (0.5–2.5%), given a subcutaneous injection of buprenorphine (0.03 mg/kg), and a single ibutton was placed within the peritoneal cavity via a 2 cm skin and abdominal wall incision 2 mm lateral to the midline. The wound was treated with antibiotic ointment (Neomycin & Polymyxin B Sulfates & Bacitracin Zinc Ointment USP), and subcutaneous buprenorphine at 6 h, and ketoprofen (5 mg/kg) at 6 h and 30 h, were administered post-operatively.

Locomotor activity data were binned every 5 min and displayed as actograms by using the Vitalview and Activeview Programs (Philips Respironics, Bend, OR). T_b actograms were created by plotting the values obtained after subtracting the mean for the entire experiment from each individual data point. The daily amplitudes of the rhythms were determined by transforming the raw data using the Morlet continuous wavelet transform, as described previously (Leise et al., 2013).

At 115 days of age, groups of G93A and control mice were placed in PhenoMaster/LabMaster metabolic cages (TSE Systems, Chesterfield, MO) using the National Mouse Metabolic Phenotyping Center (MMPC) at UMMS for non-invasive measurement of energy expenditure, food/water intake, and physical activity every 30 min over a 72 h interval.

2.3. Construction of Scholander plots (Williams College)

Telemeters (ETAF20, Data Sciences International, St. Paul, MN), were calibrated at temperatures between 20 °C and 40 °C and sterilized in povidine iodine solution overnight followed by a sterile saline rinse. At 79 days of age, mice were anesthetized, and a single telemeter was placed within the peritoneal cavity, as described for ibutton implantation, above, except for analgesia by subcutaneous meloxicam (5 mg/kg) peri-operatively and 24 and 48 h post-operatively. ECG leads from the telemeter were placed subcutaneously on either side of the heart and sutured in place.

For indirect calorimetry, air (300 ml/min) was pumped into air-tight cages, and the outflow was fed through a flow meter (Omega Engineering, Stamford, CT) and pulled through O_2 and CO_2 analyzers (AEI Technologies, Naperville, IL) at 140 ml/min, with excess flow redirected to a concentric, convoluted pathway for rerelease into the room environment. O_2 and CO_2 concentrations were sampled for 20 s every 2 min; cage temperature and atmospheric pressure were recorded every 2 min. All air put into and pulled out of the cages was dried using calcium sulfate (Drierite; W.A. Hammond Drierite Co., Xenia, OH). The adjustment of ambient temperature in the insulated cages was achieved

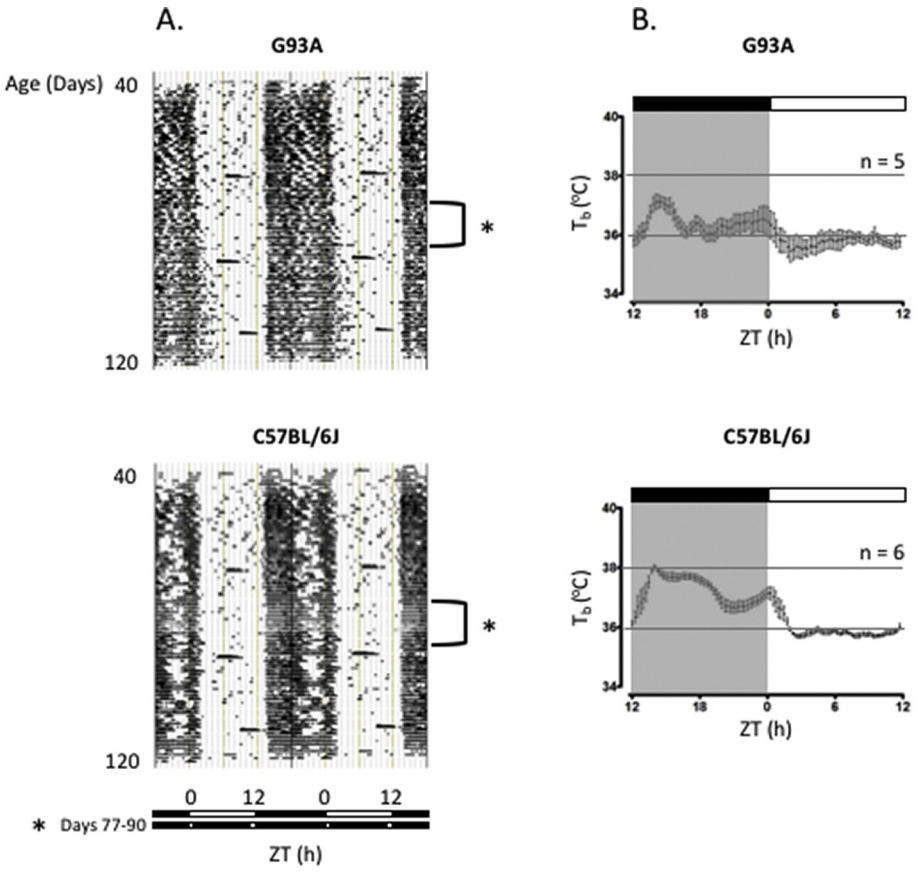

Fig. 1. Daily T_b rhythms in G93A and C57BL/6 J mice. (A). Daily T_b rhythms of a representative transgenic and control mouse portrayed in double-plotted actogram format (see text), with white and black bars at bottom denoting the timing of the external LD schedule. Brackets represent the 13-day interval of "skeleton" photoperiod (see text). The consolidated hours-long bouts of relatively high T_b during the light phase recurring every 3 weeks correspond to cage changes. (B). 24 h time course of T_b for the two groups of mice over the LD cycle, averaged over all days of recording. ZT = *zeitgeber* time, where ZT 0 represents the time of lights-on and ZT 12 the time of lights-off.

using a self-constructed temperature regulatory system consisting of copper coils of wire through which cooled antifreeze was pumped. Physiological data were collected from the telemeter's radio signal via a receiver plate placed underneath the cage (RPC-1, Data Sciences International), for 20 s every 2 min. Locomotor activity was monitored by the change in signal strength coming from the telemeter as the mouse moved about its cage, and shivering was derived from the ECG signal.

Before transfer to the metabolic cages, mice were housed at an ambient temperature of 30 °C for two weeks. Following 12 h of acclimation to the cages, data were acquired at the onset of the light phase and for the next 24 h; 1.5 h after the onset of the second light phase, ambient temperature was manually adjusted to drop 2–3 °C. Every 1.5 h thereafter, ambient temperature was dropped an additional 2–3 °C until the final 1.5 h of the light phase. Basal metabolic rate, lower critical temperature, and conductance (insulation) were calculated as previously described (see Cannon and Nedergaard, 2011). Finally, the animals were returned to 30 °C for at least two days before an acute cold stress was performed; this was initiated 1.5 h after the onset of the light phase by transfer to cages at 10 °C, after which T_b, heart rate, and activity were recorded every 2 min for 2 h.

2.4. Immunohistochemistry

Mice were euthanized with an intraperitoneal injection of ketamine (100 mg/kg) and xylazine (10 mg/kg) during the first half of the light phase of the LD cycle. Animals were perfused intracardially with heparinized (30 units/ml) 0.01 M phosphate buffered saline (PBS) followed by 4% paraformaldehyde. Brains were collected in 4% paraformaldehyde, post-fixed for 4 h and transferred to 20% sucrose at 4 °C, after which 40 μm coronal sections were cut on a sliding microtome and collected in two series in cryoprotectant and stored at 4 °C. Staining was carried out at room temperature, and all incubations and rinses (with PBS, pH 7.4, 5 min/rinse) involved gentle agitation. Free-floating sections containing the forebrain were washed in PBS, blocked for 20 min using 5% normal donkey serum (NDS, 017-000-121, Jackson ImmunoResearch Inc., West Grove, PA; or 7,332,100, Lampire Biological Labs, Pipersville, PA) in 0.3% Triton-X and PBS, and incubated for 3 h in mouse monoclonal anti-C4F6 antibody with high affinity for hSOD1 (Urushitani et al., 2007) (1:200 in 3% NDS, 0.3% Triton-X and PBS). Sections were rinsed in PBS, incubated for 2 h in a donkey anti-mouse Alexa Fluor 594 antibody (A21203, Life Technologies, Carlsbad, CA) (1:100 in 3% NDS, 0.3% Triton-X and PBS), and rinsed in PBS. All sections were mounted in PBS, air dried for 1 h and coverslipped using ProLong Gold antifade mountant (P36930, Thermo Fisher Scientific, Waltham, MA). Staining was visualized using a Zeiss Axio Imager M2 (Zeiss, Jena, Germany) and a DM IRB fluorescence microscope (Leica Microsystems, Deerfield, IL). For identification of cell groups in forebrain areas, an alternate series was stained with thionin.

2.5. Statistical analyses

ANOVAs, posthoc tests, and *t*-tests were computed using GraphPad Prism version 6 for Windows (GraphPad Software Inc., La Jolla, CA).

3. Results

3.1. G93A mice exhibit a decreased amplitude of the daily T_b rhythm

G93A (n = 5) and C57BL/6J (n = 6) mice implanted with ibuttons were maintained in a 12 h: 12 h LD cycle for recording of daily T_b and locomotor activity rhythms for up to 85 days at 22 °C. The records were graphed as "double-plotted actograms," i.e., data were plotted horizontally from left to right over the course of 48-h periods, with succeeding days stacked vertically from top to bottom, such that day n was followed by day n + 1 horizontally, succeeded by day n + 1 and n + 2

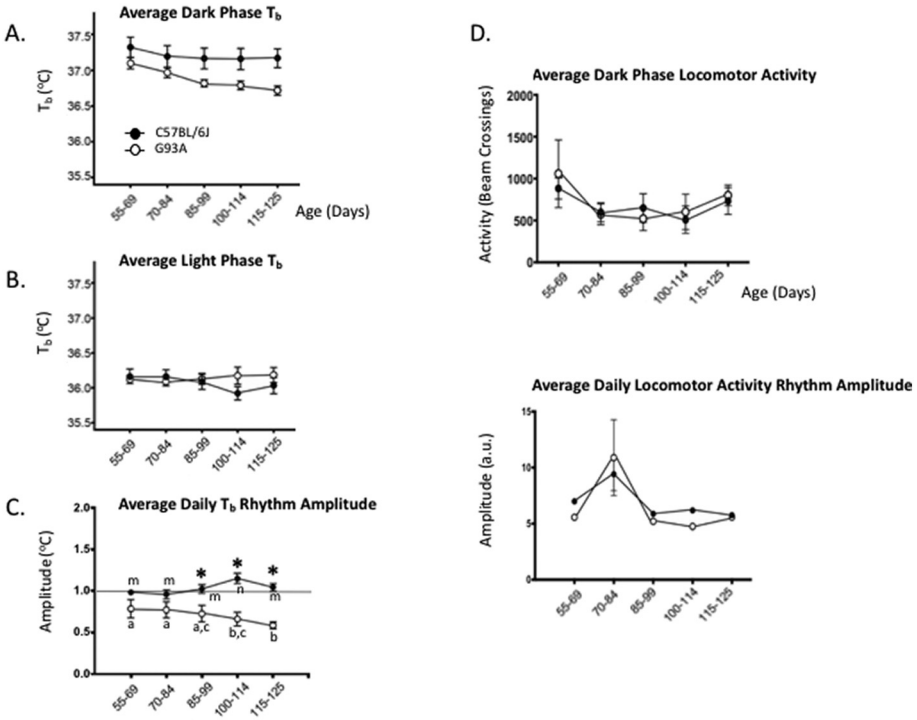

Fig. 2. Physiological measures in G93A and C57BL/6J mice. Average dark phase T_b (A), light phase T_b (B), and daily T_b rhythm amplitude (C) from 55 to 125 days of age for the two groups of mice. A repeated measures 2-way ANOVA was significant for the main effects of group and age and of the interaction (see text). Post-hoc Bonferroni comparisons indicated that the significant difference between groups first appeared during the 85–99 day age bin (*, $p < 0.01$, and later, $p < 0.001$) and that a significant decline in amplitude for the G93A group followed that time point (time points with non-identical letters represent significant within-group differences [all $p < 0.05$ or less]; time points sharing a common letter show no significant differences). There were no between-group differences in locomotor activity measures (D). G93A, open circles; C57BL/6J, closed circles; dotted line at 1 °C amplitude for illustrative purposes only.

on the next line, then by day n + 2 and n + 3, and so on. T_b actograms for representative G93A and C57Bl/6 J mice (Fig. 1A) demonstrate robust daily rhythms, with relatively high T_b during the dark (behaviorally active) phase and low T_b during the light (rest) phase of the LD cycle. For both strains, the phase and stability of synchronization to the LD cycle were comparable. Since the presence of light per se may have direct physiological effects that shape rhythm waveform (possibly masking potential defects in endogenous [circadian] mechanisms), we temporarily replaced the full LD photoperiod with a "skeleton" photoperiod, in which animals remained synchronized instead to 1 h dawn and dusk light pulses for 13 days. As shown in Fig. 1A, there was no discernable effect of the skeleton photoperiod on the rhythm (by visual inspection), indicating that light during the rest phase was not differentially suppressing T_b in the G93A mouse during that phase. One obvious difference in the actograms between strains was the appearance of an interval of relatively low T_b during the latter half of the dark phase in the C57BL/6J mouse, corresponding to inactivity on the locomotor activity actogram (not shown) and presumably representing the daily "siesta" of sleep prominent in this strain (Franken et al., 1999). These intervals were not prominent in G93A mice.

Fig. 1B plots the 24 h course of T_b over the LD cycle, averaged over all days of recording, showing qualitative differences in the T_b waveform between strains, with a blunted and more variable 24 h profile in the G93A mice. The decreased light-to-dark excursion was due to decreased dark phase T_b, not increased light phase T_b (Fig. 2A,B). In order to quantify the daily T_b rhythm amplitude, we transformed the raw T_b data using the Morlet continuous wavelet transform, allowing us to determine cycle-to-cycle peak and trough values on a circa-24 h scale without assuming sinusoidal waveforms or invariance of amplitude over time. Fig. 2C illustrates the values and trajectories of the daily T_b rhythm amplitude in the two strains, with data averaged over 14-day bins. A repeated measures 2-way ANOVA was significant for the main effects of group ($F[1,9] = 17.07$, $p < 0.003$) and age ($F[4,36] = 3.71$, $p < 0.013$) and of the interaction ($F[4,36] = 17.86$, $p < 0.0001$). Post-hoc Bonferroni comparisons indicated that the significant difference between groups first appeared during the 85–99 day age bin, with a significant decline in G93A daily T_b rhythm amplitude following that point. This decline in amplitude over the latter part of the experiment likely accounts for the variability of the G93A 24-h waveform seen in Fig. 1B, as confirmed by inspection of the G93A and C57BL/6J waveforms averaged over just the 85–99 day age bin (Supplementary Fig. 1A), with G93A actually showing less variability than control. At higher resolution, with a sampling rate of 3 min instead of 15 min, both strains exhibited the expected rise in T_b before dark onset (Supplementary Fig. 1B, conducted in a separate cohort of animals).

It is interesting that symptomatic disease onset, as assessed by the appearance of a significant difference in grip strength between the G93A and C57BL/6J mice shown in Figs. 1 and 2 also occurred during the 85–99 day age bin (Supplementary Fig. 2A). A difference in body weight appeared only much later in this cohort, after 115 days (Supplementary Fig. 2B). Most importantly, we found no significant between-strain difference in measures of locomotor activity, either as dark phase locomotor activity amounts or the daily locomotor activity rhythm amplitude (Fig. 2D); analysis of activity bouts at the ultradian scale also showed no clear differences (data not shown). Thus, decreased dark phase T_b and daily T_b rhythm amplitude cannot be ascribed to decreased locomotor activity, at least as measured by infrared sensors; in addition, the data indicate that diminished rhythm amplitude is not a general feature of G93A mice, since at least one other daily rhythm (locomotion) appears to be spared.

To test whether the decreased daily T_b rhythm amplitude in G93A mice was a fixed deficit, we repeated the experiment in a second cohort of G93A (n = 5) and C57BL/6J (n = 6) mice housed with running wheels from 45 days of age. Voluntary wheel running fully rescued the T_b rhythm amplitude defect; G93A mice tended to run more than C57BL/6J, although this difference did not reach statistical significance, and there was no between-strain difference in the amplitude of the daily wheel running rhythm (Supplementary Fig. 3). Age of onset of the decline in grip strength was no different from animals without wheels (data not shown).

Finally, to confirm the published G93A hypermetabolic phenotype with decreased body weight (Dupuis et al., 2004; Lim et al., 2014), we studied a third cohort of G93A (n = 6) and C57BL/6J (n = 5) mice using the MMPC at UMMS (ambient temperature 21.5 °C) for 72 h; the mice were between 115 and 118 days of age, at a time when the body weight of our G93A mice was nearly 10% less than controls

(Supplementary Fig. 2B). VO_2 consumption rate was about 10% higher in G93A mice at this age, both during the light and dark phases of the LD cycle (G93A, 3613 ± 57 vs C57BL/6J, 3243 ± 59 ml/h/kg during the light phase, mean ± S.E., p = 0.002; and G93A, 3954 ± 60 vs C57BL/6J, 3607 ± 74 ml/h/kg during the dark phase, p = 0.005), without a difference in food consumption during those phases (1.42 ± 0.12 vs 1.49 ± 0.10 g/12 h, p = 0.230 and 3.06 ± 0.18 vs 2.79 ± 0.16 g/12 h, p = 0.147, respectively) (Supplementary Fig. 4).

3.2. Age-dependent partial rescue of the T_b rhythm defect by thermoneutral ambient temperature

If the T_b defect in G93A mice were secondary to a disease-induced diminution in the heat generating capacity of peripheral organs (e.g., skeletal muscle, brown fat), then the need for thermogenesis by these defective tissues should be abrogated by housing under thermoneutral ambient temperature. We therefore maintained the next cohort of ibutton-implanted G93A (n = 5) and C57BL/6J (n = 4) mice in the 12 h: 12 h LD cycle but at 29 °C beginning at 45 days of age, and we compared their daily T_b rhythm amplitudes with those at 22 °C (from Fig. 2C). As expected, C57BL/6J mice showed no difference in amplitude under the two ambient conditions (Fig. 3A); a repeated measures 2-way ANOVA was significant for the main effect of age ($F[4,32] = 20.15$, $p < 0.0001$), but not of group ($F[1,8] = 0.434$, $p = 0.529$) nor of the interaction ($F[4,32] = 2.448$, $p = 0.663$). Consequently, we combined the two C57BL/6J groups for comparison with the two G93A groups housed at 22 °C and 29 °C (Fig. 3B). A repeated measures 2-way ANOVA was significant for the main effects of age ($F[4,68] = 4.498$, $p < 0.003$) and group ($F[2,17] = 17.36$, $p < 0.0001$) and of the interaction ($F[8,68] = 11.76$, $p < 0.0001$). Post-hoc Bonferroni comparisons between groups at each time point revealed that the 29 °C thermoneutral condition significantly increased the G93A daily T_b rhythm amplitude, but only during those late time bins (days 100–114 and 115–129) previously characterized as showing a progressive amplitude decline at 22 °C (see Fig. 2C); earlier time bins were unaffected by housing at 29 °C. Dark phase locomotor activity was no different at the two ambient temperatures (not shown).

3.3. Circuitry for cold-induced thermogenesis is intact at symptomatic disease onset

Lastly, we investigated the integrity of the pathways for cold-induced thermogenesis at a stage of the disease characterized by a defective daily T_b rhythm amplitude but not yet by a failure of peripheral tissue thermogenesis. G93A (n = 6) and C57BL/6J (n = 6) mice were implanted with telemeters at 79 days of age and exposed to gradually decreasing ambient temperatures from 30 °C (as described in Materials and Methods, above) when they were within the 85–99 days of age window. There were no differences in calculated basal metabolic rate (G93A, 0.57 ± 0.01 vs. C57BL/6J, 0.62 ± 0.09, VO_2 STP ml/min), lower critical temperature (the ambient temperature that marks the lower end of the thermoneutral zone) (G93A, 26.81 ± 0.26 vs C57BL/6J, 26.16 ± 0.18 °C), or the rise in metabolic rate as a function of decreasing ambient temperature (representing conductance, i.e., insulation) (Fig. 4A); T_b, locomotor activity levels, and shivering counts were not significantly different between the two strains (Fig. 4B). After recovery at 30 °C, animals were subjected to an acute cold challenge at 10 °C for 2 h, and again there were no statistically significant differences in T_b or locomotor activity levels, although the G93A mice tended to be more active than the C57BL/6J controls (Supplementary Fig. 5).

3.4. Brain hSOD1 expression is non-uniformly localized at symptomatic disease onset

Brains from G93A (n = 4, 91–100 days of age) and C57BL/6J (n = 3, 65–92 days of age) mice were processed for immunohistochemistry using a high affinity monoclonal antibody to hSOD1 (Urushitani et al., 2007). No hSOD1 staining was detected in C57BL/6 J sections, whereas G93A sections exhibited perikaryal immunoreactivity that was clearly non-uniform and localized to specific brain regions. Although we did not attempt comprehensive or quantitative mapping, it was evident that the distribution of affected regions was variable from animal to animal and included some areas implicated in thermoregulation. Among regions prominently stained were the dorsal part of the lateral septum, magnocellular preoptic nucleus,

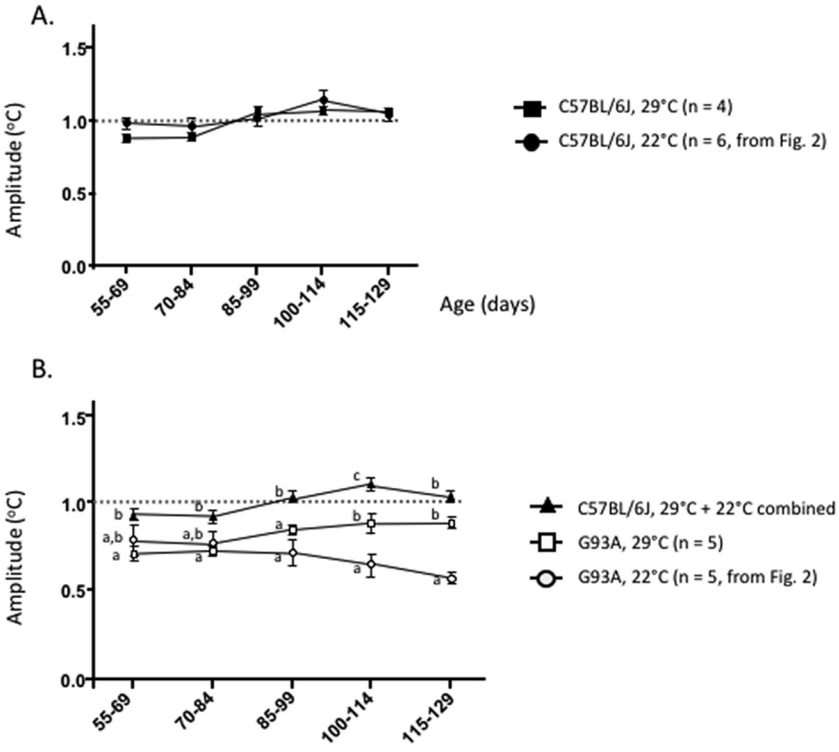

Fig. 3. Effect of thermoneutrality on daily T_b rhythm amplitudes in G93A and C57BL/6J mice. (A) No difference in daily T_b rhythm amplitude from 55 to 125 days of age in C57BL/6J mice at 29 °C and 22 °C (22 °C data from Fig. 2C). (B) Daily T_b rhythm amplitudes in groups of mice from 55 to 125 days of age at 29 °C and 22 °C (G93A 22 °C data from Fig. 2C). A repeated measures 2-way ANOVA was significant for the main effects of age and group and of the interaction (see text); significant post-hoc Bonferroni differences between groups at each time point are denoted by non-identical letters (time points at each age sharing a common letter show no significant differences; within-group differences not shown for clarity). G93A, open symbols; C57BL/6J, closed symbols; dotted line at 1 °C amplitude for illustrative purposes only.

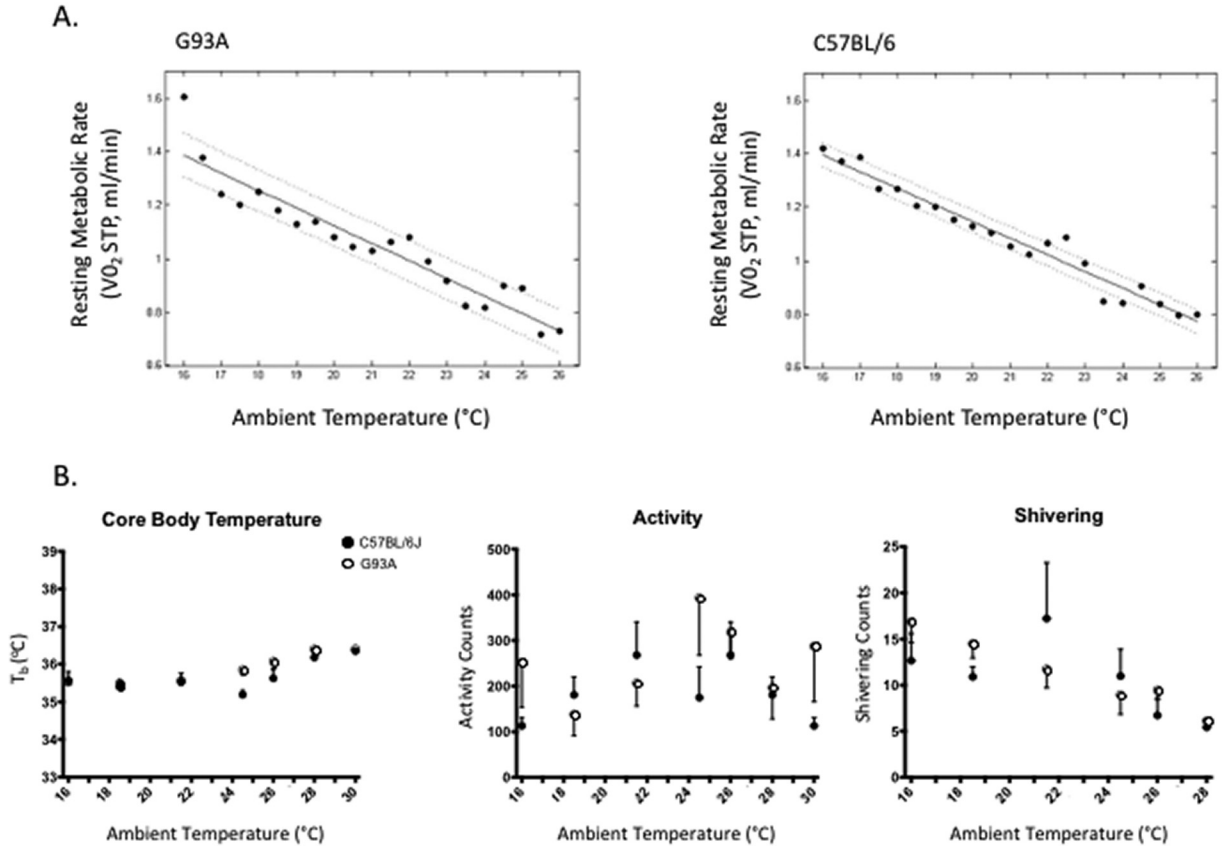

Fig. 4. Scholander curves for G93A and C57BL/6J mice. No significant between group differences in metabolic rate (A), T_b (B), locomotor activity (C), or shivering (D) as a function of decreasing ambient temperature. G93A, open circles; C57BL/6J, closed circles; dotted lines, 95% confidence limits.

dorsomedial nucleus of the hypothalamus (DMH), sub-paraventricular/retro-chiasmatic areas, and pre-mammillary nuclei, as well as others (Fig. 5).

4. Discussion

Here we have identified a defect in daily T_b regulation in the G93A murine model of ALS. The amplitude of the daily T_b rhythm is diminished in the transgenic animals, secondary to decreased T_b values during the dark (behaviorally active) phase of the LD cycle. The defect arises around the age of symptom onset (as assessed by grip strength) and cannot be accounted for by decreased levels of locomotor activity or food consumption. Our investigations implicate two, age-dependent underlying mechanisms.

In our G93A mice, an already decreased T_b rhythm amplitude progressively declines after approximately 100 days of age; this age-related defect, expressed in ambient room temperature, can be partially rescued if the animals are maintained under ambient thermoneutral conditions, suggesting that the deficit arises in part from inadequate thermogenesis by peripheral thermogenic organs. Indeed, fast-twitch muscles, which are preferentially depleted before clinical paresis in G93A mice (Hegedus et al., 2007), produce more heat than slow twitch muscles; during isometric contraction (when the only energy that is liberated is through heat), fast-twitch muscles produce 5 times more heat than slow-twitch (Barclay et al., 1993). It is tempting to propose that the modestly increased locomotor activity levels we observed in G93A mice during acute cold challenge and wheel running, although statistically not significant, might represent a kind of compensation for expending less muscular heat by generating more muscular activity (but see Vaanholt et al., 2007). Of course, brown adipose tissue (BAT), which is involved in circadian thermogenic plasticity (Gerhart-Hines et al., 2013), might also play a pathophysiological role; in G93A mice, the transgenic hSOD1 protein is expressed in BAT (by Western blot; Braun and Schwartz, unpublished observations); alternatively, or in addition, degeneration of the autonomic nervous system (Kandinov et al., 2011) could contribute to inadequate BAT activation.

However, there appears to be a second mechanism at play; thermoneutrality has no mitigating effect on the daily T_b rhythm defect at < 100 days of age, suggesting that an underlying "central" deficit is also present. Of note, when we tested the integrity of the pathways for cold-induced thermogenesis in animals at 85–99 days of age, we found that T_b was defended in G93A mice no differently than in controls, without disturbances in basal metabolic rate, lower critical temperature, or rise in metabolic rate as a function of decreasing ambient temperature. Given that a circadian "clock" in the suprachiasmatic nucleus (SCN) of the anterior hypothalamus regulates circadian rhythms of locomotor activity and T_b (Scheer et al., 2005), we posit that the most parsimonious location for a lesion that (a) disrupts the rhythm of T_b (but not of locomotion) while (b) sparing central thermoregulatory circuits would be in the output pathways from the SCN to the forebrain thermoregulatory circuitry (Lu et al., 2001; Guzmán-Ruiz et al., 2015; Vujovic et al., 2015). In particular, the output of the SCN to the DMH traverses an area called the subparaventricular zone (SPZ). Lu et al. (2001) made ibotenic acid lesions restricted to the ventral or dorsal part of the rat SPZ, which they claimed to result in differential effects on T_b and locomotor activity/sleep rhythms; lesions of the dorsal SPZ reduced the circadian T_b rhythm with relative sparing of the behavioral rhythms. Based on our immunohistochemical observations, the DMH/SPZ region is a site of hSOD1 expression at the age of symptom onset in our G93A mice. Of note, recent data in human ALS patients have implicated hypothalamic defects in the possible pathophysiology of the disease (Vercruysse et al., 2016; Gorges et al., 2017); in particular, Gorges et al. have presented MRI evidence of anterior hypothalamic atrophy.

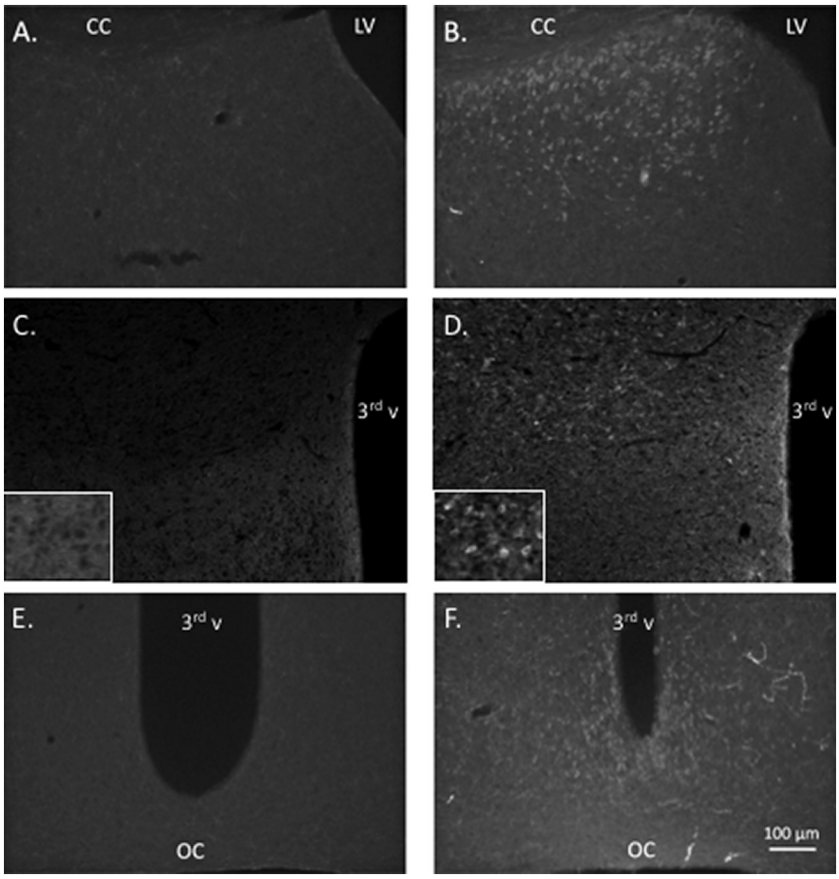

Fig. 5. Immunoreactive hSOD1 in the brains of G93A and C57BL/6J mice. Representative coronal brain sections from C57BL/6J (A, C, E) and G93A (B, D, F) mice. Levels include the dorsal part of the lateral septum (A, B), dorsomedial nucleus of the hypothalamus (C, D), and retrochiasmatic area (E, F). CC, corpus callosum; LV, lateral ventricle, 3rd v, third ventricle, OC, optic chiasm. Inset shows cytoplasmic staining in the dorsomedial nucleus of the hypothalamus.

It is interesting that providing our animals with voluntary running wheels resulted in 24-h T_b waveforms and rhythms that were indistinguishable between G93A and control mice. That G93A mice are more active wheel runners than controls has been previously reported (Bruestle et al., 2009). The mechanisms responsible for the wheel's restoration of daily T_b rhythmicity are unclear and likely to be multiple, including increased exercise, stimulation of central reward pathways, and positive feedback on SCN pacemaker amplitude (Hughes and Piggins, 2012; Novak et al., 2012; van Oosterhout et al., 2012). Running in a wheel is therapeutic for G93A mice, prolonging survival in combination with administration of insulin-like growth factor-1 (Kaspar et al., 2005).[5]

Our finding that G93A mice 85–99 days of age exhibit a normal basal metabolic rate and defense of their T_b to cold exposure can be compared to results reported by Dupuis et al. (2004), who found increased energy expenditure in 75 day old G93A and G86R mice and an inability to maintain T_b at 4 °C in 105 day old G86R mice. We note that there is a difference in disease stage between our two laboratory populations; at 75 and 95 days of age, the hypermetabolic G86R phenotype of Dupuis et al. was associated with a significantly decreased body weight, whereas our 85 to 99 day old mice had normal weights until 115 to 129 days of age. Indeed, when we tested our mice between 115 and 118 days of age, they also exhibited a 10% increase in VO_2 consumption over controls. The literature describes a wide inter-laboratory variation in the onset of decreased body weight in G93A mice (e.g., from 98 to 126 days of age in Weydt et al., 2003; Tankersley et al., 2007; and Smittkamp et al., 2008). We also note that all our mice were individually housed throughout the experiments, probably unlike other labs.

We do not know if a decreased daily T_b rhythm amplitude plays a role in the pathophysiology of disease expression and/or progression in the G93A ALS model, but an interesting possibility is that this defect might promote an internally disrupted circadian state. It is believed that metabolic health is optimized when the oscillations of circadian clocks located in body organs and tissues ("peripheral clocks") express defined, stable phase relationships to each other. The SCN plays an important role in orchestrating the stability of this oscillatory network, and the daily T_b rhythm acts as one of the critical synchronizing signals (Brown et al., 2002; Buhr et al., 2010). We speculate that decreased coupling strength (i.e., decreased amplitude of the T_b rhythm) within the network could lead to the desynchronization of peripheral clock rhythms, especially if the target organs were already compromised by disease. Interestingly, genetic loss-of-function experiments have suggested that heat-shock factor 1 (HSF1), a regulator of the heat shock response that ensures proper protein folding during stress, is necessary for the synchronizing action of the daily T_b rhythm (Saini et al., 2012); HSF1 exhibits robust circadian rhythms in its nuclear translocation and occupancy of heat-shock response elements on heat-shock protein genes (Reinke et al., 2008). In this regard, it is noteworthy that overexpression of HSF1 appears protective in an ALS murine model (Lin et al., 2013).

In sum, we find that G93A mice exhibit a dysregulated daily T_b rhythm, the mechanism of which evolves over the course of disease; initially "central," perhaps involving specific neural output pathways from the SCN, with "peripheral" superimposed later, as thermogenic organs progressively fail. On a final note, our data on G93A mice also

[5] We did record survival of our G93A cohorts to their pre-determined "death" endpoint (see Materials and Methods, above); mice maintained with running wheels or under thermoneutral conditions lived 9% longer (14 days), on average, than did those without wheels under room temperature, without a change in the timing of symptom onset as measured by grip strength. However, the G93A groups were not run concurrently and were insufficiently powered to support a definitive conclusion.

reinforce the point – as already emphasized by others (Cannon and Nedergaard, 2011) – that physiological investigations of genetically altered mice, when conducted at typical laboratory (room) temperatures, are actually not simple genotype-phenotype studies, but rather studies of the adaptation of such mice to exposure to a metabolically stressful environment.

Supplementary data to this article can be found online at https://doi.org/10.1016/j.expneurol.2018.07.008.

Funding

This work was supported in part by a research grant from the ALS Therapy Alliance to WJS and NIH grant 1R15HL120072 to SWS. Part of the study was conducted by the National Mouse Metabolic Phenotyping Center at UMMS funded by NIH grant 5U2C-DK093000 to JKK.

Conflict of Interest Statement

The authors have no potential conflicts of interest with respect to the research, authorship, and/or publication of this article.

Acknowledgements

We thank Dr. Daryl Bosco for her generous gift of anti-C4F6 antibody and Dr. Nancy Forger for facilities for immunohistochemistry.

References

Barclay, C.J., Constable, J.K., Gibbs, C.L., 1993. Energetics of fast and slow twitch muscles of the mouse. J. Physiol. 472, 61–80.
Boillée, S., Van de Velde, C., Cleveland, D.W., 2006. ALS: a disease of motor neurons and their nonneuronal neighbors. Neuron 52, 39–59.
Brown, R.H., Al-Chalabi, A., 2017. Amyotrophic lateral sclerosis. N. Engl. J. Med. 377, 162–172.
Brown, S.A., Zumbrunn, G., Fleury-Olela, F., Preitner, N., Schibler, U., 2002. Rhythms of mammalian body temperature can sustain peripheral circadian clocks. Curr. Biol. 12, 1574–1583.
Bruestle, D.A., Cutler, R.G., Telljohann, R.S., Mattson, M.P., 2009. Decline in daily running distance presages disease onset in a mouse model of ALS. NeuroMolecular Med. 11, 58–62.
Buhr, E.D., Yoo, S.H., Tahahashi, J.S., 2010. Temperature as a universal resetting cue for mammalian circadian oscillators. Science 330, 379–385.
Cannon, B., Nedergaard, J., 2011. Nonshivering thermogenesis and its adequate measurement in metabolic studies. J. Exp. Biol. 214, 242–253.
Dupuis, L., Oudart, H., Rene, F., Gonzalez De Aguilar, J.-L., Loeffler, J.-P., 2004. Evidence for defective energy homeostasis in amyotrophic lateral sclerosis: Benefit of a high-energy diet in a transgenic mouse model. Proc. Natl. Acad. Sci. U. S. A. 101, 11159–11164.
Franken, P., Malafosse, A., Tafti, M., 1999. Genetic determinants of sleep regulation in inbred mice. Sleep 122, 155–169.
Gerhart-Hines, Z., Feng, D., Emmett, M.J., Everett, L.J., Loro, E., Briggs, E.R., et al., 2013. The nuclear receptor rever controls circadian thermogenic plasticity. Nature 503, 410–413.
Gorges, M., Vercruysse, P., Müller, H.-P., Huppertz, H.-J., Rosenbohm, A., Nagel, G., Weydt, P., Petersén, Å., Ludolph, A.C., Kassubek, J., Dupuis, L., 2017. Hypothalamic atrophy is related to body mass index and age at onset in amyotrophic lateral sclerosis. J. Neurol. Neurosurg. Psychiatry 88, 1033–1041.
Gurney, M.E., Pu, H., Chiu, A.Y., Dal Canto, M.C., Polchow, C.Y., Alexander, D.D., et al., 1994. Motor neuron degeneration in mice that express a human Cu,Zn superoxide dismutase mutation. Science 264, 1772–1775.
Guzmán-Ruiz, M.A., Ramirez-Corona, A., Guerrero-Vargas, N.N., Sabath, E., Ramirez-Plascencia, O.D., Fuentes-Romero, R., et al., 2015. Role of the suprachiasmatic and arcuate nuclei in diurnal temperature regulation in the rat. J. Neurosci. 35, 15419–15429.
Hegedus, J., Putman, C.T., Gordon, T., 2007. Time course of preferential motor unit loss in the SOD1 G93A mouse model of amyotrophic lateral sclerosis. Neurobiol. Dis. 28, 154–164.
Hughes, A.T., Piggins, H.D., 2012. Feedback actions of locomotor activity to the circadian clock. Prog. Brain Res. 199, 305–336.
Ioannides, Z.A., Ngo, S.T., Henderson, R.D., McCombe, P.A., Steyn, F.J., 2016. Altered metabolic homeostais in amyotrophic lateral sclerosis: Mechanisms of energy imbalance and contribution to disease progression. Neurodegener. Dis. 16, 382–397.
Kandinov, B., Korczyn, A.D., Rabinowitz, R., Nefussy, B., Drory, V.E., 2011. Autonomic impairment in a transgenic mouse model of amyotrophic lateral sclerosis. Auton. Neurosci. 159, 84–89.
Kanning, K.C., Kaplan, A., Henderson, C.E., 2010. Motor neuron diversity in development and disease. Ann. Rev. Neurosci. 33, 409–440.
Kaspar, B.K., Frost, L.M., Christian, L., Umapathi, P., Gage, F.H., 2005. Synergy of insulin-like growth factor-1 and exercise in amyotrophic lateral sclerosis. Ann. Neurol. 57, 649–655.
Leise, T.L., Indic, P., Paul, M.J., Schwartz, W.J., 2013. Wavelet meets actogram. J. Biol. Rhythm. 28, 62–68.
Leitner, M., Menzies, S., Lutz, C., 2009. Working with ALS Mice: Guidelines for Preclinical Testing and Colony Management, Prize4Life. The Jackson Laboratory, Bar Harbor, ME, Cambridge, MA.
Lim, M.A., Bence, K.K., Sandesara, I., Andreux, P., Auwerx, J., Ishibashi, J., et al., 2014. Genetically altering organismal metabolism by leptin-deficiency benefits a mouse model of amyotrophic lateral sclerosis. Hum. Mol. Genet. 23, 4995–5008.
Lin, P.-Y., Simon, S.M., Koh, W.K., Folorunso, O., Umbaugh, C.S., Pierce, A., 2013. Heat shock factor 1 over-expression protects against exposure of hydrophobic residues on mutant SOD1 and early mortality in a mouse model of amyotrophic lateral sclerosis. Mol. Neurodegener. 8, 43.
Lu, J., Zhang, Y.-H., Chou, T.C., Gaus, S.E., Elmquist, J.K., Shiromani, P., et al., 2001. Contrasting effects of ibotenate lesions of the paraventricular nucleus and subparaventricular zone on sleep-wake cycle and temperature regulation. J. Neurosci. 21, 4864–4874.
Novak, C.M., Burghardt, P.R., Levine, J.A., 2012. The use of a running wheel to measure activity in rodents: relationship to energy balance, general activity, and reward. Neurosci. Biobehav. Rev. 36, 1001–1014.
Reaume, A.G., Elliott, J.L., Hoffman, E.K., Kowall, N.W., Ferrante, R.J., Siwek, D.F., et al., 1996. Motor neurons in Cu/Zn superoxide dismutase-deficient mice develop normally but exhibit enhanced cell death after axonal injury. Nat. Genet. 13, 43–47.
Reinke, H., Saini, C., Fleury-Olela, F., Dibner, C., Benjamin, I.J., Schibler, U., 2008. Differential display of DNA-binding proteins reveals heat-shock factor 1 as a circadian transcription factor. Genes Dev. 22, 331–345.
Robberecht, W., Sapp, P., Viaene, M.K., Rosen, D., McKenna-Yasek, D., Haines, J., Horvitz, R., Theys, P., Brown Jr., R., 1994. Cu/Zn superoxide dismutase activity in familial and sporadic amyotrophic lateral sclerosis. J. Neurochem. 62, 384–387.
Rosen, D.R., Siddique, T., Patterson, D., Figlewicz, D.A., Sapp, P., Hentat, A., et al., 1993. Mutations in Cu/Zn superoxide dismutase gene are associated with familial amyotrophic lateral sclerosis. Nature 362, 59–62.
Saini, C., Morf, J., Stratmann, M., Gos, P., Schibler, U., 2012. Simulated body temperature rhythms reveal the phase-shifting behavior and plasticity of mammalian circadian oscillators. Genes Dev. 26, 567–580.
Scheer, F.A.J.L., Pirovano, C., van Someren, E.J.W., Buijs, R.M., 2005. Environmental light and suprachiasmatic nucleus interact in the regulation of body temperature. Neuroscience 132, 465–477.
Smittkamp, S.E., Brown, J.W., Stanford, J.A., 2008. Time-course and characterization of orolingual deficits in B6SJL-Tg(SOD1-G93A)1GUR/J mice. Neuroscience 151, 613–621.
Smittkamp, S.E., Morris, J.K., Bornhoff, G.L., Chertoff, M.E., Geiger, P.C., Stanford, J.A., 2014. SOD1-G93A mice exhibit muscle-fiber-type-specific decreases in glucose uptake in the absence of whole-body changes in metabolism. Neurodegener. Dis. 13, 29–37.
Speakman, J., 1997. Factors influencing the daily energy expenditure of small mammals. Proc. Nutr. Soc. 56, 1119–1136.
Tankersley, C.G., Haenggeli, C., Rothstein, J.D., 2007. Respiratory impairment in a mouse model of amyotrophic lateral sclerosis. J. Appl. Physiol. 102, 926–932.
Taylor, J.P., Brown Jr., R.H., Cleveland, D.W., 2016. Decoding ALS: from genes to mechanism. Nature 539, 197–206.
Tsuda, T., Munthasser, S., Fraser, P.E., Percy, M.E., Rainero, I., Vaula, G., Pinessi, L., Bergamini, L., Vignocchi, G., Crapper McLachlan, D.R., Tatton, W.G., St George-Hyslop, P., 1994. Analysis of the functional effects of a mutation in *SOD1* associated with familial amyotrophic lateral sclerosis. Neuron 13, 727–736.
Urushitani, M., Ezzi, S.A., Julien, J.P., 2007. Therapeutic effects of immunization with mutant superoxide dismutase in mice models of amyotrophic lateral sclerosis. Proc. Natl. Acad. Sci. U. S. A. 104, 2494–2500.
Vaanholt, L.M., Garland Jr., T., Daan, S., Visser, G.H., 2007. Wheel-running activity and energy metabolism in relation to ambient temperature in mice selected for high wheel-running activity. J. Comp. Physiol. B. 177, 109–118.
van Oosterhout, F., Lucassen, E.A., Houben, T., van Leest, H.T., Antle, M.C., Meijer, J.H., 2012. Amplitude of the SCN clock enhanced by the behavioral activity rhythm. PLoS ONE 7, e39693.
Vercruysse, P., Sinniger, J., El Oussini, H., Scekic-Zahirovic, J., Dieterlé, S., Dengler, R., Meyer, T., Zierz, S., Kassubek, J., Fischer, W., Dreyhaupt, J., Grehl, T., Hermann, A., Grosskreutz, J., Witting, A., Van Den Bosch, L., Spreux-Varoquaux, O., the GERP ALS Study Group, Ludolph, A.C., Dupuis, L., 2016. Alterations in the hypothalamic melanocortin pathway in amyotrophic lateral sclerosis. Brain 139, 1106–1122.
Vujovic, N., Gooley, J.J., Jhou, T.C., Saper, C.B., 2015. Projections from the subparaventricular zone define four channels of output from the circadian timing system. J. Comp. Neurol. 523, 2714–2737.
Weydt, P., Hong, S.Y., Kliot, M., Möller, T., 2003. Assessing disease onset and progression in the SOD1 mouse model of ALS. Neuroreport 14, 1051–1054.
Weydt, P., Pineda, V.V., Torrence, A.E., Libby, R.T., Satterfield, T.F., Lazarowski, E.R., et al., 2006. Thermoregulatory and metabolic defects in Huntington's disease transgenic mice implicate PGC-1a in Huntington's disease neurodegeneration. Cell Metab. 4, 349–362.
Zetterström, P., Stewart, H.G., Bergemalm, D., Jonsson, P.A., Graffmo, K.S., Andersen, P.M., et al., 2007. Soluble misfolded subfractions of mutant superoxide dismutase-1s are enriched in spinal cords throughout life in murine ALS models. Proc. Natl. Acad. Sci. U. S. A. 104, 14157–14162.